Possibility of a superfluid phase in a Bose condensed excitonic state

P. Wachter, B. Bucher,* and J. Malar
Laboratorium für Festkörperphysik, ETH Zürich, 8093 Zürich, Switzerland
(Received 11 March 2003; revised manuscript received 1 December 2003; published 2 March 2004)

In the condensed excitonic phase of intermediate valent $TmSe_{0.45}Te_{0.55}$ the thermodynamic properties have been measured. The heat conductivity and the thermal diffusivity have been obtained between 300 K and 1.5 K and between ambient pressure and 17 kbar (1.7 GPa), as a first experiment of its kind. Pressure and temperature are used to navigate in three different phases of the material, the intermediate valent semiconducting phase, the condensed excitonic phase, and the intermediate valent metallic phase. In the condensed excitonic phase the heat conductivity λ increases strongly below about 20 K, suggesting a superfluid phase for the lowest temperatures. In a solid under equilibrium conditions this has never been seen before. Also the thermal diffusivity a strongly increases below 20 K, giving evidence for second sound. The quotient $\lambda/\rho a$ represents the specific heat, which thus can be calculated, for the first time as a function of pressure. When entering the condensed excitonic phase under pressure and from high temperatures (100 K–250 K), the Dulong-Petit value of the specific heat drops precipitously to about half its value. Also this phenomenon is unprecedented. The entropy has been calculated from the heat capacity and the Debye temperature has been obtained as a function of pressure. In addition the longitudinal sound velocity has been measured under pressure and as a function of temperature. Entering the excitonic phase the sound velocity drastically increases by about a factor 2.

DOI: 10.1103/PhysRevB.69.094502 PACS number(s): 67.90.+z, 63.20.Kr, 65.40.−b, 65.40.Ba

I. INTRODUCTION

TmSe and TmTe are some well known rare earth chalcogenide compounds[1] which crystallize in the fcc rocksalt structure and, with the exception of a narrow miscibility gap between $0.2<x<0.4$, can be alloyed in the whole concentration range[2,3] of $TmSe_{1-x}Te_x$. It has been found[4–6] that for a certain region $0.5<x<0.68$ these compounds exhibit under pressure and at low temperature the phenomenon of exciton condensation in the sense of an excitonic insulator, as predicted by Mott[7] (1961). The Tm chalcogenides are not the only system in which this phenomenon has been observed, also in $Sm_{1-x}La_xS$,[8–10] $Sm_{1-x}Tm_xS$,[10,11] YbO, and YbS.[8] This type of exciton condensation (after 1990) is so far only observed in rare earth compounds.

The phenomenon of exciton condensation has been sought for more than 30 years and the literature is full of claims that exciton condensation has been found. But there were always other, conventional explanations possible. Also in our first publication on this topic,[4] besides exciton condensation, an alternative explanation of the experimental findings was offered. There it was found that the resistivity of some $TmSe_{1-x}Te_x$ alloys at low temperatures increased with increasing pressure. But only a Hall effect measurement under pressure in a large magnetic field, to separate the normal from the anomalous Hall effect,[5] revealed that the resistivity increase was due to a freezing out of charge carriers, supporting the proposal of exciton formation and condensation under pressure. In the meantime the finding of new materials and measurements of the transport, lattice and magnetic properties have become routine. The prerequisites for exciton condensation are an intermediate valent condition[5] (usual found in rare earths) and a certain range of carrier concentration prior to exciton condensation. This carrier concentration should not be too high to avoid screening the Coulomb interaction between electrons and holes, and not too low to enable the formation of enough excitons which then can condense. This is usually achieved by alloying an intermediate valent metal with a semiconductor, such as TmSe and TmTe to form $TmSe_{1-x}Te_x$. Within the range $0.5<x<0.68$ $TmSe_{0.45}Te_{0.55}$ has shown the largest effects, so we concentrate on the following in this composition.

Intermediate valence provides us due to $f-d$ hybridization with a narrow f valence band and as consequence with a large effective mass $(50m_e-100m_e)$. In exciton formation this will be a hole mass, reducing the diffusive mobility of excitons and thus increasing their stability.[6] We believe that this is the main reason for this new type of exciton condensation. Also an indirect band gap between the $4f$ band and $5d$ band is of advantage so the exciton condensation can be of the Bose-type with the help of phonon interaction.[12] Thus we have a positive and a negative charge coupled via the Coulomb interaction and in principle, a created or destroyed phonon for momentum conservation.

In order to lay a basis for the understanding of the new thermodynamical properties we show in Fig. 1 the principal part of the band structure of $TmSe_{0.45}Te_{0.55}$. The conduction band in the [100] direction is made up of $\Delta_{2'}$ $5d$ wave functions, which for symmetry reasons in the fcc crystal structure have a minimum at the X point of the Brillouin zone. The band is several eV wide and the bottom of the band has some admixture of f character. The valence band is an occupied narrow $4f$ band, which due to hybridization has acquired some $5d$ character. Symmetry considerations show that the maximum of the f band is at the Γ point of the Brillouin zone. The heavy masses in the f band and the narrow gap $\Delta E=130$ meV (Ref. 6) (at ambient conditions) make the material behave like an indirect semiconductor, which also has an activated electrical resistivity. We have measured an excitonic state, which basically also has a localized $5d$ character, with a binding energy $E_B=70$ meV (Ref. 6) below the $5d$ conduction band. The full line repre-

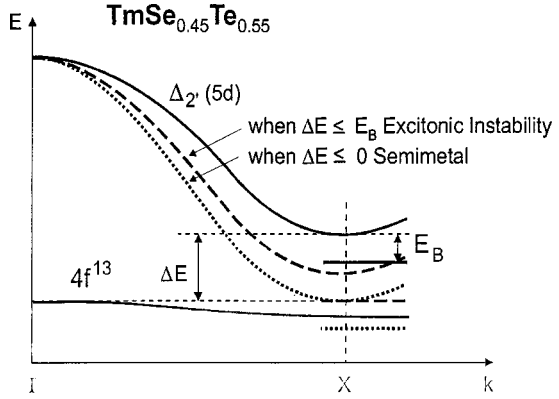

FIG. 1. The main points of the band structure of $TmSe_{0.45}Te_{0.55}$ in the [100] direction. E_B is the exciton binding energy and ΔE is the energy required to promote a quasilocalized f-electron into a $5d$ state.

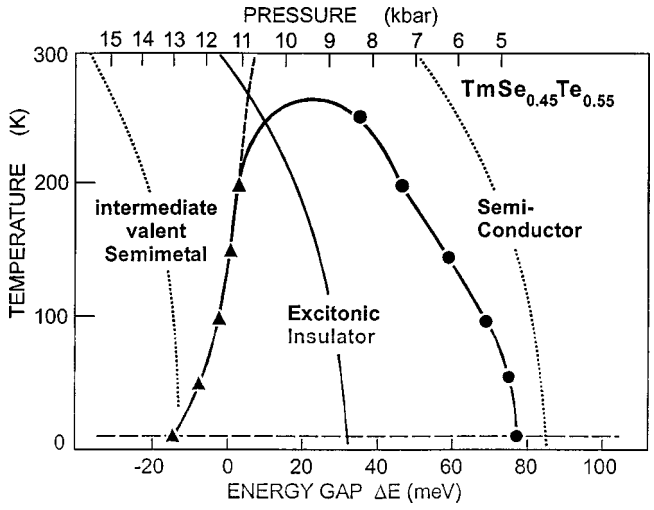

FIG. 2. The excitonic phase diagram of $TmSe_{0.45}Te_{0.55}$. Experimental points designated by symbols. ''Isobars'' in the semiconducting and semimetallic phase are shown as dotted lines, whereas an ''isobar'' entering the excitonic phase is shown by a full line. The short dashed line separates semiconductor from semimetal.

sents the band structure of $TmSe_{0.45}Te_{0.55}$ at ambient conditions.

The result of external pressure can be viewed as to widen the $5d$ band with respect to its center of gravity and it thus reduces the energy gap ΔE. We assume in first approximation that the exciton binding energy E_B remains constant when the bottom of the $5d$ band is moving.

At low temperature and with increasing pressure a first anomaly can be expected when $\Delta E = E_B$ which is at about 5 kbar. The dashed curve in Fig. 1 is appropriate for this pressure. A $4f$ electron at the Γ-point can enter the excitonic state at X with the same energy and can create the bound state of an exciton with the remaining heavy hole at Γ. Of course the momentum Γ–X must be supplied by an interaction with a phonon. With further increase of pressure more and more excitons are formed. At 8 kbar this process is completed and the excitonic level has reached the bottom of the dispersing f band at X. At 8 kbar essentially one f electron per formula unit has the chance to become an exciton and with this large concentration of excitons an overlap of exciton orbits and exciton condensation can and will occur. Of course, individual excitons have only a short lifetime. At 8.5 kbar e.g., and at low temperatures we have estimated the concentration of excitons to be about 3.9×10^{21} cm^{-3}, about 25% of the atomic density.[6] The simultaneous formation and condensation of so many excitons leads to a new ground state of matter, the excitonium, an expression coined by Mott,[7] inasmuch as no excitation e.g., with light is necessary to form the excitons. At the same pressure and temperature where excitons condense one observes a large lattice expansion of 1.6%,[4,6] which presumably is due to the formation of a huge amount of excitonic $5d$ orbits, which are much larger than the $4f$ orbits prior to exciton formation.[6] Besides, excitons as electric dipoles repel each other at short distances, i.e., at high concentration, augmenting the former argument. It is thus that the material becomes extremely hard during exciton formation and condensation.[6] This lattice expansion is isostructural,[4] i.e., the fcc structure is pertained and no superstructure is observed. Also other rare earth compounds in which exciton condensation has been observed[8–11] remain in the fcc phase upon exciton formation as has been checked explicitly on $Sm_{1-x}Tm_xS$ (Refs. 10, 11) and YbO and YbS,[13] in the latter case even up to 300 kbar.

A further increase of pressure above 8 kbar first compresses only the excitonic state until a new situation is achieved (dotted curve in Fig. 1) when the bottom of the $5d$ band at X approaches the top of the $4f$ band at Γ. More and more of the remaining f electrons now spill into the $5d$ band, screening the Coulomb interaction between the electrons and holes until finally the excitons destabilize, suddenly increasing the electron concentration in the $5d$ band in a first order transition. The hybridization between the $4f$ and $5d$ band results in an intermediate valent semimetallic state.

In Fig. 2 we show the temperature–pressure phase diagram of the condensed excitonic phase. At temperatures above about 250 K, e.g., 300 K, one crosses with increasing pressure (upper scale going towards the left) between 10 and 11 kbar the (short)-dashed line, separating the semiconductor–semimetallic phase. At lower temperatures instead, one enters with increasing pressure at first the condensed excitonic state (above 5 kbar) and leaves the excitonic state between 11 and 15 kbar to enter the semimetallic phase. Such a phase diagram has been predicted by Mott[7] and Kohn.[14] In the lower abscissa the energy gap ΔE is plotted, negative values refer to the metallic state.[6] Either the pressure scale (top) or the energy gap scale (bottom) is nonlinear. Of interest and experimentally simply accessible are the isobars, where in a clamped pressure cell at a chosen pressure the temperature is decreased and thus one navigates in the pressure–temperature phase diagram.

An isobar should be a vertical line in the diagram of Fig. 2. However, upon cooling the pressure transmitting medium contracts and the pressure relaxes somewhat. The pressure is monitored in the cell and thus an isobar at 12 kbar at 300 K looks like the full line in Fig. 2. It will be of relevance in the whole paper that e.g., an isobar, starting at about 7 kbar or

below at 300 K, will not enter the excitonic phase but remain in the semiconducting phase. An isobar starting at about 14 kbar or above at 300 K will remain in the metallic phase. This is indicated by two dotted lines in the phase diagram.

II. EXPERIMENTAL ARRANGEMENT

To measure the heat conductivity λ and the thermal diffusivity a, bar shaped single crystals of $TmSe_{0.45}Te_{0.55}$ of about 1.5 mm length were placed in a Cu–Be pressure cell withstanding pressures up to 20 kbar. Either small evaporated minute Au–Chromel or Au–Ni calibrated thermocouples were used between one end of the crystal and the other end in contact with a Cu heat sink, thus creating also a differential thermometer of 0.1 K precision at the lowest temperatures. A Mäander-type thin film heater was placed at one end of the crystal. The pressure inside the cell was monitored by a calibrated manganin coil. The thermovoltage per degree at the most insensitive liquid He temperatures is only about 0.2 μV/K, which yields for 0.1 K temperature difference only about 20 nV. After an amplification of 10^5 the signal was about 2 mV with a large noise background. The noise has been reduced by a designed and homebuilt active unity gain Bessel low pass filter of eighth order. This means that for higher frequencies than the desired one the amplitudes get diminished as f^{-8} instead of as f^{-1} like in a conventional passive R–C filter. After that the noise level was appreciably less than the signal. The heat input ΔT of typically less than 1 K was periodically with the so-called ''temperature wave method'' (Berman[15] and references quoted therein) which, for the thermal diffusivity, quantitatively eliminates the effect of radial heat loss into the pressure fluid. A longitudinal shunting of the heat conductivity of the crystal by the pressure fluid is negligible since the heat conductivity of the liquid is lower by orders of magnitudes. Details of the arrangement are described in Ref. 16. The pressure cell could be cooled in a bath cryostat down to about 1.5 K. However, not all measurements (practically at each kbar) were carried to this low temperature because of the high He and time consumption. Heat conductivity and thermal diffusivity were measured automatically in steps of 1 K. Pressure was applied at room temperature in a power press and the cell was clamped at the desired pressure. To our knowledge it is the first time that heat conductivity and thermal diffusivity have been measured under pressure and down to low temperatures.

The heat conductivity λ is obtained in a measurement where the temperature difference between both ends of the crystal with length L and cross section A is monitored for a certain rate of heat input: $Q/t=\lambda\ A\ \Delta T/L$, with $\Delta T>0$ (steady state equation of heat flow). The thermal diffusivity a is measured essentially with the same arrangement, but it is a dynamical method. The sample is heated also periodically and the temperature along the sample varies with the same period but with diminished amplitude. Moreover, as the temperature wave travels along the sample with finite velocity there is a varying phase relationship. Measurement of the amplitude decrement and the phase difference with a lock-in technique enables the diffusivity a to be determined. As the temperature distribution throughout the sample varies with time, the complete differential equation of heat flow is involved: $\partial\ T/\partial\ t=a*\nabla^2 T$, with $a=\lambda/\rho c_v,\rho$ being the density and c_v the specific heat. The heat conductivity had good precision and a good reproducibility. The error bars in Figs. 3 and 4 refer only to the absolute value of heat conductivity and thermal diffusivity at low temperatures, respectively. The relative precision is much higher. Both types of measurements were taken point by point, but automatically at each degree.

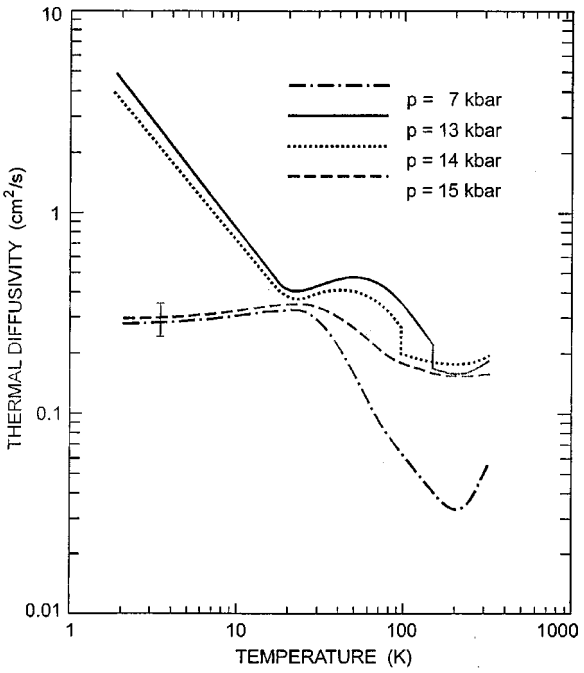

FIG. 3. The thermal diffusivity a of $TmSe_{0.45}Te_{0.55}$ for various pressures as a function of temperature. Dotted and full line in the excitonic region, dashed in the metallic region, and dashed–dotted in the semiconducting phase.

The longitudinal sound velocity v has been measured in the same clamped pressure cell as a function of pressure and temperature. An ultrasound transducer was glued to one end of the bar shaped crystal and in a pulse-multiple echo experiment over the length of the crystal the sound velocity has been determined.

III. RESULTS AND DISCUSSION

A. Heat conductivity and thermal diffusivity

The motivation to measure heat conductivity and thermal diffusivity in the phase of excitonic condensation is due to a long-standing controversy amongst theorists. Keldish and Kopaev 1965[17] and Kozlov and Maximov 1966[18] proposed that in a condensed excitonic phase at low temperatures a superthermal current could exist. They used an analogy to superconductivity where, as in our case, two charged particles strongly couple to a phonon. This was opposed by Zittartz 1968,[19] who claimed that the heat conductivity in a condensed excitonic state would be quite normal. Since only

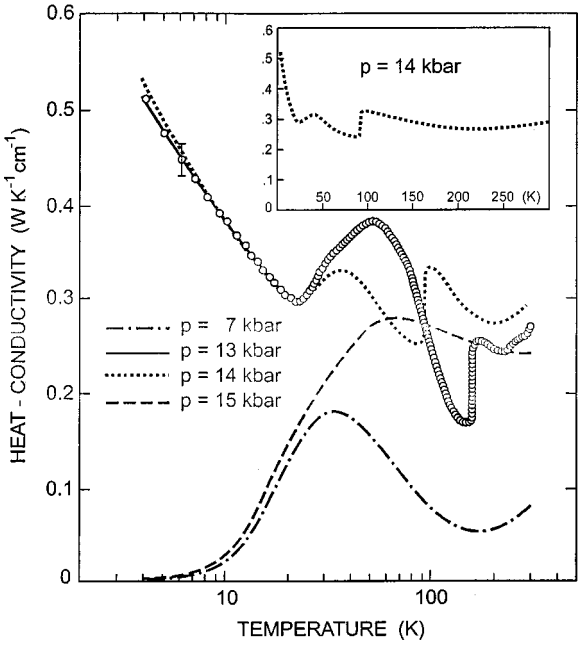

FIG. 4. The heat conductivity λ of $TmSe_{0.45}Te_{0.55}$ for various pressures as a function of temperature. Dotted and full line in the excitonic region, dashed in the metallic region, and dashed–dotted line in the semiconducting phase. The inset shows the heat conductivity at 14 kbar in a linear scale. The actual points of measurements are shown in the curve for 13 kbar, measured automatically at all degrees.

in recent years the phenomenon of a stable exciton condensation was realized[4–6,8–11] the time has come to settle the dispute.

The equation of heat conductivity is $\partial Q/\partial t = -\lambda \text{ grad } T$ with $\lambda = 1/3\ Cv\ell$; C is the heat capacity per volume $C = \rho c_v$ with ρ the density and c_v being the specific heat for constant volume. v is the velocity of sound and ℓ the mean free path. Thus $\lambda = 1/3\rho c_v v\ \ell$ or $\lambda = 1/3\rho c_v v^2 \tau$, τ being the collision time. The thermal diffusivity $a = \lambda/\rho c_v$ so that $a = 1/3 v\ \ell$. The independent measurement of λ and a thus permits the evaluation of $c_v = \lambda/a\rho$. In reality we should use c_p instead of c_v, but the volume change in a solid is small and in this case complex (the volume expands when entering the excitonic phase[6]), so we refrain from doing so. Since both entities λ and a are measured with pressure we obtain also for the first time in a solid the specific heat under pressure in the whole temperature range from 1.5 K towards 300 K (see below).

Generally speaking the various contributions to the heat conductivity λ are additive: $\lambda_{tot} = \lambda_{el} + \lambda_{ph} + \lambda_{ex}$. λ_{el} is the metallic part given by the Wiedemann-Franz ratio, λ_{ph} is the phonon part, and λ_{ex} the excitonic contribution. The sound velocity v and the density ρ will not have an excessive temperature dependence outside the excitonic region, thus the temperature dependence of the heat conductivity due to phonons, λ_{ph}, is mainly depending on the specific heat c_v and on the mean free path for phonon scattering ℓ_{ph}. With the same argumentation the thermal diffusivity a will be mainly proportional to the mean free path ℓ_{ph}. The dependence of the mean free path and heat conductivity on temperature is described in many textbooks, e.g., Ref. 20. In short, ℓ_{ph} will increase with decreasing temperature because the density of phonons decreases and we have Umklapp processes involving 3 phonons. At low temperatures λ_{ph} reaches the geometrical dimensions of the sample and becomes temperature independent.

In Fig. 3 we show the thermal diffusivity a as a function of temperature. At 7 kbar (dashed–dotted curve) we remain in the semiconducting phase outside the excitonic region (see dotted curve in Fig. 2). The curve follows the description above and is mainly proportional to the mean free path ℓ_{ph} for phonon scattering, reaching for temperatures below about 20 K the linear dimensions of the crystal. At 15 kbar we stay in the metallic (semimetallic) phase (dashed curve), again outside the excitonic region. The thermal diffusivity follows also the temperature dependence of the mean free path, this time for electron–phonon scattering. Since the concentration of electrons in a metal is largely temperature independent, it is again the phonon scattering which determines a. The weak maximum near 30 K in the thermal diffusivity has no explanation at present.

Before discussing the excitonic region of a in Fig. 3 we look at Fig. 4 for the heat conductivity λ, also outside the excitonic region. We have derived above that the heat conductivity follows mainly the temperature dependence of c_v and ℓ_{ph}. Since c_v definitely will go towards zero for $T \to 0$, the heat conductivity outside the excitonic region generally displays a maximum near 50 K, as well for the insulating case at 7 kbar as also for the metallic case at 15 kbar. The difference of the heat conductivity near 300 K for both cases is due to the electronic part of the heat conductivity in the metallic state and it corresponds roughly to the Wiedemann-Franz relation. Thus the heat conductivity and the thermal diffusivity behave as expected with pressure, as well in the insulating as in the metallic phase, which gives confidence in the experimental method and shows that possible heat losses into the pressure fluid are indeed negligible. (We show only a selection of curves in order not to overload the pictures and the reader.)

We continue the discussion of the heat conductivity in Fig. 4, but now in the excitonic region at 13 kbar and 14 kbar. The first thing which is unexpected are the downward jumps in a first order transition when entering the excitonic phase. Consulting Fig. 2 it is obvious that at different pressures one enters the excitonic phase at different temperatures. At these temperatures and pressures one enters the insulating excitonic phase mainly from the semimetallic phase, thus with a metal–insulator transition. It is conceivable that the downward jumps in λ reflect the loss of the electronic part of the heat conductivity. But measuring an isobar at 11 kbar one enters the excitonic region from the semiconductor phase (see Fig. 2), but the downward jump in λ is of the same size as the jumps when entering the excitonic region from the semimetal. Here we have to realize that many phenomena occur simultaneously at the excitonic phase transition. We have stated above, that λ_{tot} is the sum of many contributions, all of which can and will change at the phase transition, such as λ_{ex}, when excitons suddenly appear and simultaneously condense with a density of about[6]

4×10^{21} cm^{-3}. Also λ_{ph} may change due to a renormalization of the phonon spectrum when certain phonons get bound or coupled in the formation of the excitons. On the other hand the thermal diffusivity a in Fig. 3 displays at the same temperatures an upward jump. Since $a=1/3\,\ell_{ph}v$, we may wonder which of the two entities dominates the upwards jumps. In fact it is the sound velocity v which increases sharply when entering the excitonic phase, as a separate measurement reveals (see below). So in the above formula $\lambda=\rho c_v a$, when entering the excitonic phase λ jumps downwards, a jumps upwards, thus c_v must also jump downwards and not because of the metal–insulator transition. We propose that many phonons suddenly get absorbed or bound in the formation and condensation of excitons and no longer carry heat as independent oscillators or running waves. This creates a new quasiparticle, the exciton–polaron with a density of about 10^{21} cm^{-3}. However, there are still enough other phonons present at each temperature to ensure a conduction of heat. This will be discussed later on in connection with the specific heat.

We may speculate what are the heat carriers in the various regions of the phase diagram? For temperatures above the phase boundary of exciton condensation certainly phonons, or in case of a metal, also electrons will carry the heat. At the temperatures and pressures of exciton condensation the heat conductivity λ becomes strongly reduced in a first order transition, and this in spite of the fact that now in addition to phonons also excitons may carry some heat. In our opinion this is only possible when the phonons, as main carriers of the heat, are strongly reduced in their number because many phonons are absorbed or bound by the excitons. In the temperature range 20 K to 250 K the exciton–polarons (possibly self-trapped) as quasiparticles do not yet contribute significantly to the heat conductivity. In the region of condensed excitons but above about 20 K the heat is carried now by the free phonons and the quasiparticles, but the phonons are still dominant, as shown in Fig. 4. Here λ still displays its maximum due to the competition of an increase in mean free path of phonons and a decrease of the specific heat. But below about 20 K the heat conductivity and its increase towards lower temperatures is not at all phononlike and we have to assume that now the exciton–polaron quasiparticles take over completely.

An increase in heat conductivity for T going to zero is certainly very new and unexpected. In the inset of Fig. 4 we show in a linear scale the heat conductivity for 14 kbar and the rise at low temperatures is spectacular. There is only one case prior to these results where the heat conductivity rises just as drastically and this is in the case of superfluidity in ^{4}He (and in ^{3}He),[21] but there in a first order transition, accompanied by the famous λ-anomaly in the specific heat at 2.2 K. We propose that in our case we also have a superthermal current in the two-fluid model, where the superfluid part increases gradually towards zero temperature. However, a λ-anomaly in the specific heat as in the first order Bose-Einstein transition in ^{4}He is here not to be expected and also not found. Thus in the whole phase diagram we have in fact two condensation phenomena, at first an exciton condensation which forms a liquid and then below about 20 K an increasing part of superfluidity. At the moment it is not known how much heat input the superfluid phase supports before it quenches. In superconductivity a large current will also destroy the superconducting state.

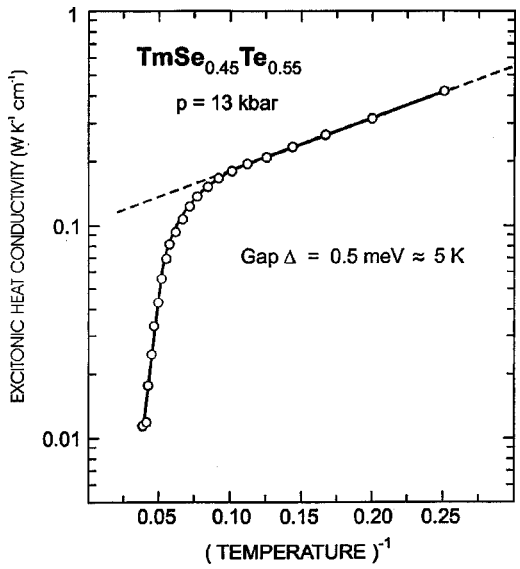

FIG. 5. Excitonic part of the heat conductivity λ_{ex} at 13 kbar, shown in an Arrhenius plot.

The proposed evidence of superfluidity within the condensed excitonic state necessitates a certain excitation spectrum of (other) quasiparticles,[21] namely rotons or vortices. In the low temperature excitonic region below about 20 K $\lambda_{tot}=\lambda_{ph}+\lambda_{ex}$, where λ_{ph} represents the heat conductivity due to uncoupled phonons. The heat conductivity due to phonons alone is proportional to T^3 and can be neglected compared to λ_{ex} at low temperatures, having only an influence near 20 K (where it is not important). Thus we obtain for λ_{ex}, the excitonic part of the heat conductivity, an Arrhenius law for the increase of the heat conductivity towards zero temperature $\lambda_{ex}\propto\exp\Delta/k_BT$. This is shown in Fig. 5 at 13 kbar. We find an activation energy or gap Δ of 0.5 meV or about 5 K. The application of heat in the heat conductivity experiment can excite quasiparticles, e.g., rotons, in which case the roton gap would be 5 K, which is the right order of magnitude. In superfluid ^{4}He the roton gap is 8.65 K.[22] So the exciton–polaron quasiparticles seem to exhibit a similar phenomenon as phonons alone in a classical superfluid.

Now we discuss the thermal diffusivity a in the excitonic region at low temperatures. Here we go back to Fig. 3. At the same temperature where λ increases below about 20 K, also a increases, even faster than λ. We have argued before that the reason for a largely temperature independent thermal diffusivity below about 20 K in the **non**-excitonic region is that the mean free path for phonon scattering ℓ_{ph} has reached the geometrical dimensions of the sample.[20] Why then, in the excitonic region at 13 kbar and 14 kbar, the dimensions of the crystal do not seem to be important now? Just as in a He superfluid (but not only there) heat can be transferred not only via phonon–phonon scattering in a diffuse manner, but ballistically via a highly directional quantum mechanical wave, the second sound, aimed in the direction of the tem-

perature gradient. This can also be the reason that the thermal diffusivity a can increase strongly in the excitonic state at low temperatures, where heat is now carried by the exciton–polaron quasiparticles. And in fact a has to increase strongly because c_v, which is proportional to λ (see above) still has to go to zero for $T \rightarrow 0$ even in the excitonic phase. Since $c_v = \lambda/\rho a$, so a must rise faster with decreasing temperature than λ. Thus we propose a strong similarity between the properties of a classical superfluid as in He II, where heat is being carried by phonons, with our solid system consisting of a condensed exciton–polaron quasiparticle liquid.

Thus we have three independent pieces of evidence for the appearance of a superfluid phase in the condensed excitonic phase: The heat conductivity seems to become quite large with deceasing temperature, even infinite for $T \rightarrow 0$. A roton spectrum with a gap of about 0.5 meV seems to exist, and the second sound may be responsible for the sharp increase of the mean free path below about 20 K. In any case the phenomena are unprecedented in a solid, but not unexpected theoretically.[17,18]

B. Specific heat and Debye temperature

The specific heat curves are computed from the independent measurements of λ and a as $c_v = \lambda/\rho a$ and they are actually obtained from point by point measurements of λ and a. We have used above in simplified terms the heat conductivity $\lambda = 1/3 \rho c_v v\, \ell$. If we concentrate on the insulating phase we have $\lambda_{\mathrm{ph}} = 1/3 \rho c_v \ell_{\mathrm{ph}}$. c_v and ℓ_{ph} depend on T and Θ, the Debye temperature, and a more explicit modified formula of the heat conductivity is given by Berman[15] as

$$\lambda_{\mathrm{ph}} = 3 n k_B v \left(\frac{T}{\Theta}\right)^3 \int_0^{\Theta/T} \ell(x)_{\mathrm{ph}} \frac{x^4 e^x}{(e^x - 1)^2} dx,$$

with n being N/V and x being θ/T. Closer inspection of this formula reveals that it corresponds exactly to the simpler formula even without the standard low and high temperature approximations in the derivation of the (Debye) specific heat. The problem is that ℓ_{ph} appears in the integral and in fact ℓ_{ph} stands for the sum of all mean free paths of the various carriers of heat. Even if they exchange heat fast enough to establish a local temperature, it is by no means trivial to pull ℓ_{ph} in front of the integral. In order to test the effect of ℓ_{ph} in front of the integral we made a worst case scenario and computed $c_v = \lambda/\rho a$ even of a metal. Here the problem is that heat is mainly carried by the electrons, but the specific heat is dominated by the phonons. The electron contribution to the specific heat is only manifest in the γ term at very low temperatures. We have taken the data of copper from the tabulated and measured values of λ and a.[23] The result is shown in Fig. 6 (the original data even go above the melting point of copper). In the figure we also have plotted the well-known specific heat of copper from a classical c_v measurement from textbooks. The agreement is impressive. But it shows that also in the thermal diffusivity the same mechanisms work as in the heat conductivity.

In fact we are not the only ones who have computed the specific heat from the measured λ and a. The specific heat c_v in a function of pressure up to 30 kbar, but only at 300 K, has been computed for polytetrafluoroethylene (Teflon).[24] Having gained confidence in the method we compute the specific heat $c_v = \lambda/\rho a$ from the combination of the values independently measured for $TmSe_{0.45}Te_{0.55}$ in Figs. 3 and 4 and plot them in Fig. 7. At first we discuss the results outside the excitonic region, i.e., at 7 kbar for the semiconducting phase and at 15 kbar for the metallic case.

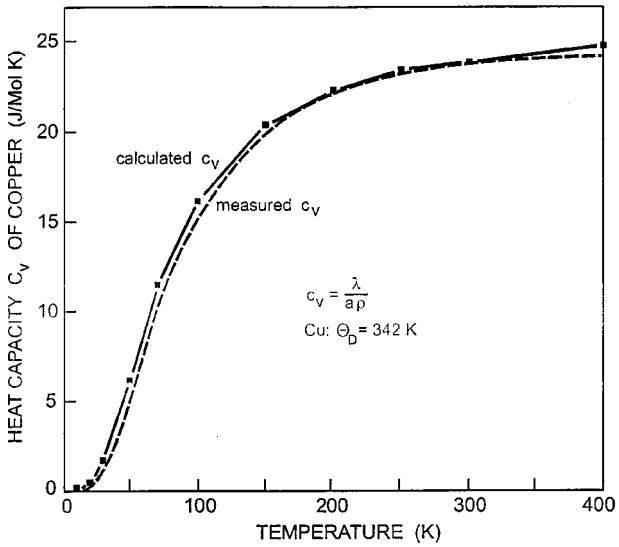

FIG. 6. Comparison of the calculated heat capacity of copper as $c_v = \lambda/a\rho$ with a directly measured heat capacity (Ref. 22).

The specific heat turns out to be quite normal, having a Dulong-Petit value at 300 K of about 50 J/mol K, which is the expected value for a solid with diatomic molecules. Since there exists the possibility of a magnetic order in

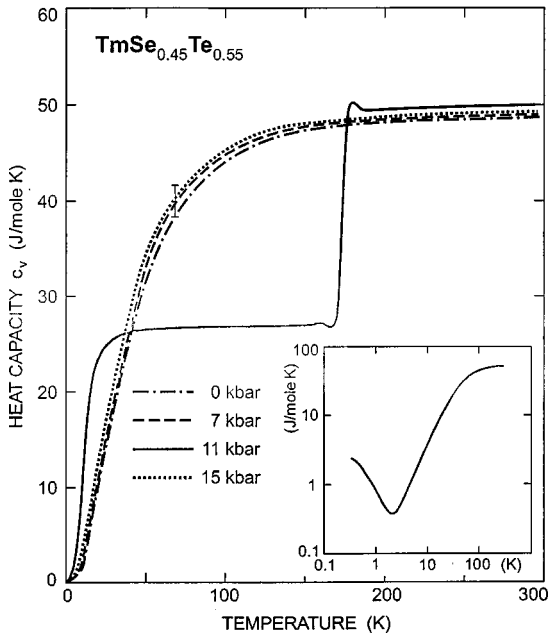

FIG. 7. Calculated heat capacity of $TmSe_{0.45}Te_{0.55}$. Dashed–dotted curve from a direct measurement of the heat capacity (Ref. 24), also shown in a log–log scale in the inset.

$TmSe_{0.45}Te_{0.55}$ below about 1 K in the insulating phase, we had a conventional specific heat measurement at ambient pressure being made (p=0 kbar in Fig. 7) (Ref. 25) as a calibration for high and low temperatures. Although it turned out that there is a magnetic order near 0.2 K as defined by a peak in the specific heat, the influence of magnetic order at 300 K is remarkably small. The expected theoretical Dulong-Petit value of 49,88 J/mol K is experimentally very well obtained. Our calculated c_v values at 7 kbar and 15 kbar needed only a small adjustment, near 100 K which we take into account by an error bar.

However, in the excitonic phase with, e.g., 11 kbar again something unexpected takes place. We recall the unusual jumps downwards in the heat conductivity curves in Fig. 4 when entering the excitonic phase and the upward jumps in the thermal diffusivity at the same temperatures in Fig. 3. In the quotient for c_v these jumps add and result in the large drop of about a factor 2 in the specific heat when entering the excitonic phase in a first order transition. This jump in c_v is of about the same size for all pressures measured in the excitonic phase. We have chosen to show the specific heat at 11 kbar in the excitonic region, because generally the point by point measurement is not always so good as to reveal a small λ-like anomaly, which seems to exist before the drop of c_v. It is also observed that in the low temperature region the specific heat in the excitonic region is shifted towards lower temperatures, indicating a shift of the Debye temperature Θ towards lower temperatures. The specific heat curve in the excitonic region is certainly very unusual. We might add, that a plot of c_v/T vs T, being proportional to the entropy, reveals that the missing area, e.g., $[c_v(0\ \text{kbar}) - c_v(11\ \text{kbar})]/T$ between 170 K and 50 K is about the same as the additional area $[c_v(11\ \text{kbar}) - c_v(0\ \text{kbar})]/T$ between 50 K and 1.5 K, thus there is no loss of entropy in the excitonic transition.

The specific heat is a very basic measurement and one has no room for exotic interpretations. The Dulong-Petit value depends only (in a nonmagnetic material) on $c_v = 3Nk_B = 49.88$ J/mol K for a solid consisting of diatomic molecules. The drop of c_v by nearly a factor of 2 when entering the excitonic phase occurs still in the Dulong-Petit region. For temperatures above the excitonic phase this region is dominated by phonons. However, a metal–insulator transition when entering the excitonic phase from the semimetallic state at 13 kbar and 14 kbar is not manifest in the specific heat. At the excitonic phase transition excitons simultaneously appear and condense. At 8.5 kbar we have estimated the exciton density to be about 4×10^{21} cm^{-3}, 25% of the atomic density.[6] At 11 kbar as in Fig. 7 the density of excitons is even larger and the excitons are already compressed. We proposed for the heat conductivity that every appearing exciton absorbs a phonon and forms an exciton–polaron quasiparticle, at first phonons with a wave vector Γ–X (see Fig. 1), then with decreasing wave vector the more excitons appear. In this situation less and less phonons apparently act as free oscillators. If the excitons–polarons have a very low mobility due to the large inertia of the heavy hole mass, it is thus possible and it is our proposal, that these quasiparticles (in the temperature range 20–250 K) do not contribute significantly to the heat conductivity, but the remaining free phonons still can carry the (reduced) heat conductivity. The same reduction in phonons or modes as free oscillators due to the formation of the exciton quasiparticles, is responsible for the drop in the specific heat.

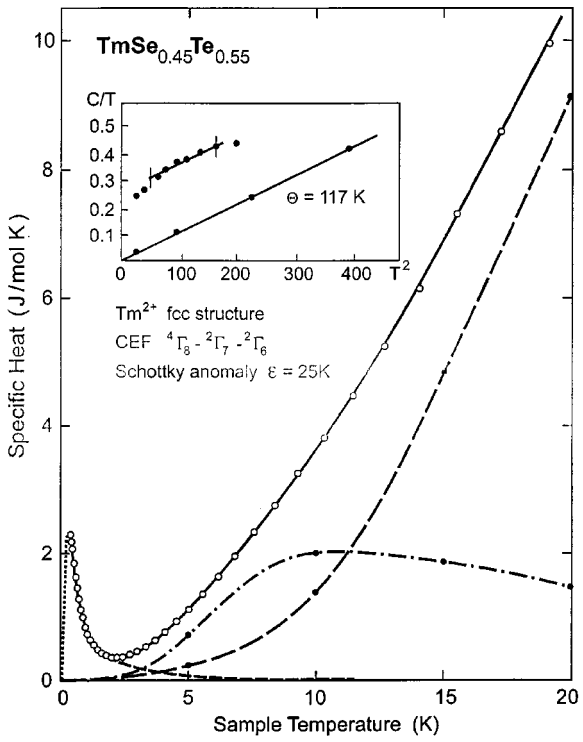

FIG. 8. Direct measurement of c_v at ambient pressure (round symbols) (Ref. 24). Dotted curve extrapolation to $T=0$. Dotted and small dashed curve magnetic contribution to c_v (Ref. 27). Dotted–dashed curve is the Schottky anomaly contribution of crystal field levels to c_v. Long dashed curve is the measured c_v (Ref. 24) minus magnetic contribution minus Schottky contribution and is thus the phonon part of c_v alone. In the inset is the phonon contribution in a c/T versus T^2 plot with $\Theta = 117$ K. The other curve in the inset is from the directly measured c_v (Ref. 24).

Already by visual inspection of Fig. 7 we see that at 0 kbar, 7 kbar, and 15 kbar the Debye temperature Θ is about the same, whereas with 11 kbar, and generally for pressures in the excitonic phase, Θ is much lower. To estimate Θ from the specific heat measured at ambient pressure down to 0.3 K (Ref. 25) is not so simple, because there is a magnetic order at about 0.2 K, which is probably of the antiferromagnetic type, as expected for an intermediate valent compound[1] (see inset of Fig. 7).

In Fig. 8 we show the low temperature part of the measured specific heat at ambient pressure for $TmSe_{0.45}Te_{0.55}$ between 0.3 K and 20 K.[25] In spite of the fact that in a double log plot as in the inset of Fig. 7, c_v is linear between 5 K and 13 K with slope 3, a closer inspection of c_v/T vs T^2 reveals (inset Fig. 8 upper curve) that the straight line would not go through zero. The reason is, of course, the magnetic contribution and the Schottky anomaly due to crystal field effects in the Tm ions. Tm^{2+} as in TmTe has a well-known crystal field splitting $^4\Gamma_8(0) - {}^2\Gamma_7(10\ \text{K}) - {}^2\Gamma_6(16\ \text{K})$ of the $J=7/2$ ground state and a T_N of 0.23 K.[26] A fit of the mea-

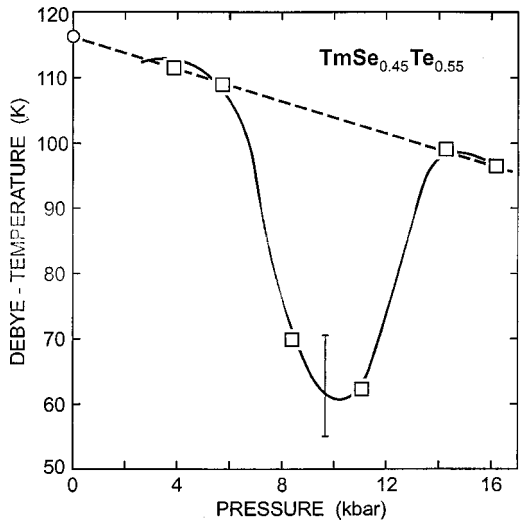

FIG. 9. Computed Debye temperatures from the calculated heat capacity curves. Round symbol from the direct measurement of c_v at ambient pressure (Ref. 24).

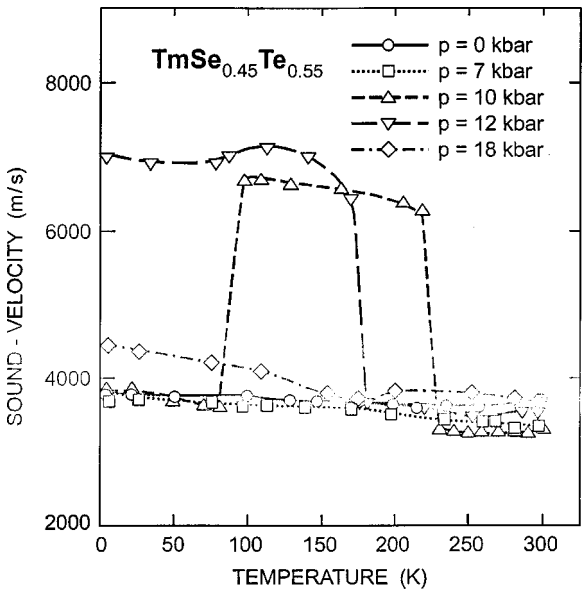

FIG. 10. Sound velocity measurements of $TmSe_{0.45}Te_{0.55}$ for various pressures as a function of temperature.

sured c_v of TmTe using these data is not too successful.[27] In our case with $TmSe_{0.45}Te_{0.55}$ we have first a smaller lattice constant than in pure TmTe (which can be taken into account for the crystal field splitting using an a^5 power law), and second we have an admixture of Tm^{3+} in the sense of intermediate valence. Thus we take an experimentally determined crystal field splitting ε of 25 K and compute a Schottky anomaly due to crystal field splitting, plotted in Fig. 8. Also a magnetic exchange contribution to the specific heat can be calculated,[28] using a magnetic ordering temperature of 0.23 K as in TmTe,[26] which is also shown in Fig. 8. Thus subtracting the Schottky and the exchange contribution from the measured c_v and plotting the remaining specific heat as c_v/T versus T^2 (inset of Fig. 8 lower curve) a Debye temperature Θ of about 117 K can be computed for $TmSe_{0.45}Te_{0.55}$.

Such a detailed analysis of the specific heat as in the case of ambient pressure for a directly measured c_v cannot be made for the computed high pressure specific heat curves as in Fig. 7. But here we learn from the inset of Fig. 8 (upper curve) that between 5 K and 13 K the specific heat as measured is linear in a c_v/T versus T^2 plot yielding the correct Debye temperature Θ. Thus we can show in Fig. 9 the Debye temperature of $TmSe_{0.45}Te_{0.55}$ as a function of pressure.

How can Θ change so drastically in one and the same material? Here we have to look at Fig. 1 again. The first excitons appear when $\Delta E = E_B$, which occurs at a pressure of about 5 kbar. But at the same time and with increasing pressure and the generation of more and more condensed excitons, phonons with smaller and smaller wave number get absorbed or couple to the excitons forming exciton–polarons. But the heat conductivity at low temperatures, but above 20 K, is still assured because it is carried mostly by low energy-low k phonons. But we have another problem with the lowering of Θ in the excitonic region. In the Debye approximation Θ is connected with $\omega_{\max}$, so this entity decreases also. In the simplest model $\omega = (f/m)^{1/2}$, and since we cannot change the masses, a decreasing ω means a reduction of the spring constants f, resulting in a softening of the material. However, we have shown[6] that during exciton condensation the compound hardens appreciably, the compressibility tending to zero. These two incompatible results force us to leave the simplified Debye model. We have to use a more realistic phonon dispersion, than the simple $\omega \propto k$. Thus, as we have stated already in the chapter of heat conductivity and thermal diffusivity, a strong renormalization of the phonon spectrum occurs in the condensed excitonic state.

C. Sound velocity

The longitudinal sound velocity of $TmSe_{0.45}Te_{0.55}$ has been measured in the same pressure cell and with the same bar shaped single crystal as used in the other thermodynamic measurements. An ultrasound transducer has been glued to one end of the crystal and with a multiple echo from the other end of the crystal over the known length of the crystal the sound velocity could be obtained. For various pressures this is shown in Fig. 10. The main features are that the sound velocity v_L for pressures outside the excitonic phase, i.e., at 0 kbar, 7 kbar, and 18 kbar exhibits no special temperature dependence, except in the semimetallic phase at 18 kbar it is somewhat larger than in the insulating phases. However, best seen for 12 kbar when entering the excitonic phase around 180 K the sound velocity increases sharply by about a factor 2. With 10 kbar we enter the excitonic phase near 240 K (see Fig. 2). We observe again the jump with an increase of about a factor 2, but near 90 K the pressure loss in the cell was just the size to have a re-entrant transition to the nonexcitonic phase, a unique phenomenon, which gives support to the measurement.

It thus becomes clear, as stated already in the chapter about thermal diffusivity, that the upward jumps in the thermal diffusivity a in Fig. 3 when entering the excitonic phase indeed are caused by the jumps in the sound velocity. In

addition the maximum in the sound velocity at 12 kbar and similar pressures directly contributes to the maximums of the thermal diffusivity in the excitonic phase in Fig. 3. Here we have to remark, that the sound velocity v used in the formulas for heat conductivity and thermal diffusivity is in reality a weighted average of sound velocities $1/3(v_L+2v_T)$. But since v_L is about a factor 3 larger than v_T it is mainly v_L which dominates v.

The sound velocity is closely related to the bulk modulus B and its inverse the compressibility κ. For a cubic material the bulk modulus B depends on the elastic moduli c_{ij} as $B=\frac{1}{3}(c_{11}+2c_{12})$. On the other hand the elastic modulus $c_{11}=\rho\, v^2_{L\,[100]}$ and $c_{12}=\rho\,(v^2_{L\,[100]}-2v^2_{T2\,[110]})$. Assuming again that in general v_L is about 3 times v_{T2} we get the simplified relation $B\sim\rho v_L^2$. In the excitonic phase of $TmSe_{0.45}Te_{0.55}$ we get a two times larger sound velocity v_L and therefore a four times larger bulk modulus B or a 4 times smaller compressibility κ. The material indeed gets appreciably harder in the excitonic state.

In Ref. 6 (Fig. 4) we have shown with a measurement of the lattice constant as a function of pressure at 1.5 K (elastic neutron scattering through the pressure cell) that between 5 kbar and 8 kbar the lattice constant remained practically unchanged during exciton condensation. This means that the compressibility would be close to zero. Putting a maximal error bar through the points of measurement a bulk modulus of $B=20$ GPa outside the excitonic region and a bulk modulus of 70 GPa in the excitonic region could be obtained. With the results from the sound velocity measurements of Fig. 10 we calculate a bulk modulus of $B=24$ GPa outside the excitonic region and a bulk modulus of 100 GPa in the excitonic region. So both types of measurements agree reasonably well and confirm the fact that during exciton condensation the material becomes extremely hard.

We have offered above two explanations for this phenomenon: the electron of the exciton enters a $5d$-like orbit, which is much larger than the original $4f$ orbit it came from, and this against increasing pressure. Or the excitons, being electric dipoles, repel each other at short distances, especially for large concentrations, creating a counter pressure to the applied pressure.

We still have to explain why in the excitonic region the Debye temperature is reduced (Fig. 9), but the sound velocity (Fig. 10) is increased. In the Debye model the sound velocity is the slope of a linear phonon dispersion curve whose maximum frequency $\omega_{\max}$ determines the Debye temperature Θ. Generally speaking a material with a lower Debye temperature has a lower sound velocity and a lower bulk modulus (compare copper and lead). In order to explain a lower $\omega_{\max}$ together with a higher sound velocity and a larger bulk modulus, we have to leave the simple Debye model. If we use instead of a dispersion curve for bare LA phonons, $\omega\propto\sin(ka/2)$, a new dispersion curve of an exciton–polaron quasiparticle we can in the excitonic state simultaneously reduce the maximum frequency and increase the initial slope, the sound velocity. The dispersion is then no longer a simple sinus function. The dispersion of such an exciton–polaron quasiparticle is treated in textbooks, e.g., Ref. 29. We think

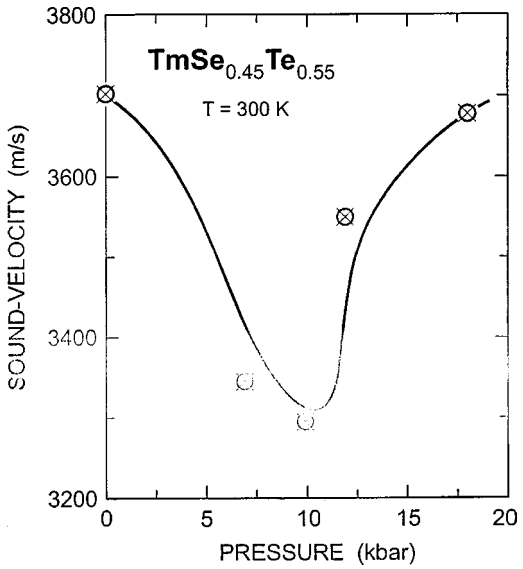

FIG. 11. Sound velocity measurements of $TmSe_{0.45}Te_{0.55}$ at 300 K as a function of pressure.

that such a dispersion exists for our special conditions, and it just means, as stated already several times, that the phonon spectrum will be greatly renormalized in the excitonic state. This will have to be confirmed by inelastic neutron measurements under pressure and low temperature.

Looking now in Fig. 10 at an isotherm at 300 K and using the given pressures, we obtain Fig. 11. Now this is a measurement at room temperature and has nothing to do with excitonic condensation. Here we find a minimum of the sound velocity with increasing pressure, that is inverse to what we have discussed in the excitonic range. The equations of bulk modulus and sound velocity now show a softening of the bulk modulus with increasing pressure and a minimum of the bulk modulus near 10 kbar. We recall that the compressibility κ is the inverse of the bulk modulus, so κ has a maximum at about 11 kbar. This agrees very well with a direct measurement of the compressibility of $TmSe_{0.45}Te_{0.55}$ (Ref. 1) (not the same crystal), giving again confidence into the sound velocity measurements. At 300 K the softening of the bulk modulus is due to a change of the degree of valence mixing with pressure.[1]

IV. CONCLUSION

In this paper we have measured for the first time the heat conductivity λ, thermal diffusivity a, and longitudinal sound velocity v as a function of pressure and temperature on a material $TmSe_{0.45}Te_{0.55}$, known to exhibit exciton condensation under pressure and at low temperatures. The specific heat c_v was inferred through $c_v=\lambda/a\rho$.

For the first time there has been given evidence that in a Bose condensed excitonic state an ever increasing heat conductivity exists below 20 K with tendency to become infinite for $T\rightarrow 0$. Such a phenomenon has only been observed for ^{4}He II, the prototype for superfluidity below 2.2 K. Thus we use this analogy to postulate superfluidity also in our material. Our measurements give also evidence for a roton gap of

0.5 meV. The second sound seems to be responsible for an increase of a, the thermal diffusivity beyond the limit of surface scattering below 20 K. These results are unprecedented and for the first time could mark the stable existence of a superfluid phase in a solid.

In the excitonic phase we propose that phonons strongly couple to the excitons, forming exciton–polaron quasiparticles. The specific heat drops precipitously by about a factor 2, presumably due to a corresponding loss in uncoupled phonons or modes, which indicates a strong phonon renormalization, a unique situation. As a consequence also the Debye temperature drops dramatically in the excitonic state in spite of the fact that the sound velocity, and with it the bulk modulus, sharply increase. The latter is related to a nearly incompressible solid during exciton condensation. Thus again, a strong renormalization of the phonon spectrum in the excitonic phase is necessary. A coupling of excitons with phonons, an exciton–polaron quasiparticle, would yield a dispersion which simultaneously has a larger initial slope (the sound velocity) and a lower $\omega_{\max}$ than a conventional bare phonon dispersion.

At last it should be mentioned that exciton condensation and superfluidity has also been reported for a Bose-Einstein condensed excitonic gas.[30–33] Here a strong picoseconds long laser pulse creates excitons. The important experimental claims try to proof the exciton condensation by measurement of the exciton recombination luminescence and its time and spatial distribution. Superfluidity during these short times is mostly stated and brought in connection with shifts in the luminescence spectrum, referring to the theoretical paper of Keldysh and Kopaev[17] which predicts superfluidity for a condensed excitonic state.

The greatest difference to the other mentioned papers is that we have exciton condensation as an equilibrium process and we can perform many time consuming experiments in this condition. The density of exciton quasiparticles in our material system is with about 10^{21} cm^{-3} (or about 25% of the atomic density) orders of magnitude larger than the typically 10^{16}–10^{17} cm^{-3} in the laser excited materials. This large concentration of condensed excitons even influences the heat conductivity and the specific heat, which has never been seen before.

ACKNOWLEDGMENT

The authors thank very much H.P. Staub for technical help and preparing the figures.

*Permanent address: HSR Hochschule für Technik Rapperswil/ Switzerland.

[1] P. Wachter, *Handbook on the Physics and Chemistry of Rare Earths*, edited by K. A. Gschneider, Jr., L. Eyring, G. H. Lander, and G. R. Choppin (Elsevier Science, Amsterdam, 1994), Vol. 19, Chap. 132, p. 177.

[2] E. Kaldis, B. Fritzler, E. Jilek, and A. Wisard, J. Phys. (Paris) **40**, C5-366 (1979).

[3] E. Kaldis and B. Fritzler, Prog. Solid State Chem. **14**, 95 (1982).

[4] J. Neuenschwander and P. Wachter, Phys. Rev. B **41**, 12693 (1990).

[5] B. Bucher, P. Steiner, and P. Wachter, Phys. Rev. Lett. **67**, 2717 (1991).

[6] P. Wachter, Solid State Commun. **118**, 645 (2001).

[7] N. Mott, Philos. Mag. **6**, 287 (1961).

[8] P. Wachter, J. Alloys Compd. **225**, 133 (1995).

[9] P. Wachter, A. Jung, and P. Steiner, Phys. Rev. B **51**, 5542 (1995).

[10] A. Jung and P. Wachter, Physica B **230-232**, 725 (1997).

[11] U. Schärer, A. Jung, and P. Wachter, Physica B **244**, 148 (1998).

[12] B. I. Halperin and T. M. Rice, Rev. Mod. Phys. **40**, 755 (1968).

[13] A. Jayaraman, *Handbook on the Physics and Chemistry of Rare Earths*, edited by K. A. Gschneidner, Jr. and L. Eyring (North–Holland, Amsterdam, 1979), Vol. 2, Chap. 20, p. 575.

[14] W. Kohn, in *Many Body Physics*, edited by C. de Witt and R. Balian (Gordon & Breach, New York, 1968).

[15] R. Berman, in *Thermal Conduction in Solids*, edited by B. Bleane, D. W. Sciama, and D. H. Wilkinson (Clarendon, Oxford, 1976).

[16] J. Malar, Ph.D. thesis ETH Zürich, 2000 (unpublished).

[17] L. V. Keldish and Yu. V. Kopaev, Sov. Phys. Solid State **6**, 2219 (1965).

[18] A. N. Kozlov and L. A. Maksimov, Sov. Phys. JETP **23**, 88 (1966).

[19] J. Zittartz, Phys. Rev. **165**, 612 (1968).

[20] K. H. Hellwege, *Introduction to Solid State Physics* (Springer Verlag, Berlin, Heidelberg, New York, 1976).

[21] D. R. Tilley and J. Tilley, in *Superfluidity and Superconductivity*, edited by D. F. Brewer (Adam Hilger, Bristol and New York, 1990), p. 35.

[22] D. G. Henshaw and A. D. W. Woods, Phys. Rev. **121**, 1266 (1961).

[23] Y. S. Touloukian, R. W. Powell, C. Y. Ho, and M. C. Nicolaou, in *Thermal Diffusivity* (IFI/Plenum, New York, 1973).

[24] P. Anderson and G. Bäckström, High Temp. - High Press. **4**, 101 (1972).

[25] The authors are most grateful to Professor A. Junod, University of Geneva, Switzerland, ($T>1$ K) and to Dr. Ch. Bergemann, ETH Zürich, Switzerland, ($T>0.3$ K) for performing heat capacity measurements at ambient pressure.

[26] H. R. Ott, B. Lüthi, and P. S. Wang, in *Valence Instabilities and Related Narrow Band Phenomena*, edited by R. Parks (Plenum, New York, 1977), p. 289.

[27] T. Matsumura, Y. Haga, Y. Nemoto, S. Nakamura, T. Goto, and T. Suzuki, Physica B **206-207**, 380 (1995).

[28] W. Stutius, Phys. Kondens. Mater. **10**, 152 (1969).

[29] J. N. Hodgson, in *Optical Absorption and Dispersion in Solids* (Butler and Tanner, London, 1970).

[30] A. E. Bulatov and S. G. Tikhodeev, Phys. Rev. B **46**, 15058 (1992).

[31] E. Fortin, S. Fafard, and A. Mysyrowicz, Phys. Rev. Lett. **70**, 3951 (1993).

[32] M. R. Matthews, B. P. Anderson, P. C. Haljan, D. S. Hall, C. E. Wieman, and E. A. Cornell, Phys. Rev. Lett. **83**, 806 (2000).

[33] K. W. Madison, F. Chevy, W. Wohlleben, and J. Dalibard, Phys. Rev. Lett. **84**, 2056 (2000).